

# The nerve growth factor alters calreticulin translocation from the endoplasmic reticulum to the cell surface and its signaling pathway in epithelial ovarian cancer cells

CAROLINA ANDREA VERA<sup>1</sup>, LORENA ORÓSTICA<sup>1</sup>, FERNANDO GABLER<sup>2</sup>, ARTURO FERREIRA<sup>3</sup>, ALBERTO SELMAN<sup>4</sup>, MARGARITA VEGA<sup>1,4</sup> and CARMEN AURORA ROMERO<sup>1,4,5</sup>

<sup>1</sup>Laboratory of Endocrinology and Reproduction Biology, Clinical Hospital, University of Chile, Santiago;

<sup>2</sup>Department of Pathology, School of Medicine, San Borja Arriarán Clinical Hospital, University of Chile, Santiago;

<sup>3</sup>Program of Immunology, Institute of Biomedical Sciences (ICBM), Faculty of Medicine, University of Chile, Santiago;

<sup>4</sup>Department of Obstetrics and Gynecology, School of Medicine, Clinical Hospital, University of Chile, Santiago;

<sup>5</sup>Advanced Center for Chronic Diseases (ACCDiS), University of Chile, Santiago, Chile

Received November 2, 2016; Accepted February 20, 2017

DOI: 10.3892/ijo.2017.3892

**Abstract.** Ovarian cancer is the seventh most common cancer among women worldwide, causing approximately 120,000 deaths every year. Immunotherapy, designed to boost the body's natural defenses against cancer, appears to be a promising option against ovarian cancer. Calreticulin (CRT) is an endoplasmic reticulum (ER) resident chaperone that, translocated to the cell membrane after ER stress, allows cancer cells to be recognized by the immune system. The nerve growth factor (NGF) is a pro-angiogenic molecule overexpressed in this cancer. In the present study, we aimed to determine whether NGF has an effect in CRT translocation induced by cytotoxic and ER stress. We treated A2780 ovarian cancer cells with NGF, thapsigargin (Tg), an ER stress inducer and mitoxantrone (Mtx), a chemotherapeutic drug; CRT subcellular localization was analyzed by immunofluorescence followed by confocal microscopy. In order to determine NGF effect on Mtx and Tg-induced CRT translocation from the ER to the cell membrane, cells were preincubated with NGF prior to Mtx or Tg treatment and CRT translocation to the cell surface was determined by flow cytometry. In addition, by western blot analyses, we evaluated proteins associated with the CRT translocation pathway, both in A2780 cells and human ovarian samples. We also measured NGF effect

on cell apoptosis induced by Mtx. Our results indicate that Mtx and Tg, but not NGF, induce CRT translocation to the cell membrane. NGF, however, inhibited CRT translocation induced by Mtx, while it had no effect on Tg-induced CRT exposure. NGF also diminished cell death induced by Mtx. NGF effect on CRT translocation could have consequences in immunotherapy, potentially lessening the effectiveness of this type of treatment.

## Introduction

Ovarian cancer is the seventh most common cancer among women worldwide and the first cause of death due to a gynecological malignancy (1). This disease causes ~150,000 deaths every year (1) and it has a mortality rate between 17 and 47% 5 years after the diagnosis (2,3). Approximately 90% of ovarian cancers are of epithelial origin, known as epithelial ovarian cancer (EOC) (4). EOC is typically asymptomatic at early stages, and therefore it is usually diagnosed at advanced stages, when it responds poorly to therapy (4). Although many patients respond to the first line of treatment, surgery and chemotherapy, recurrence is developed in ~90% of advanced cases (5). Due to this poor response, it is important to find new and more effective treatments. Immunotherapy is designed to boost the body's natural defenses against cancer (6) and it appears to be a promising option against EOC (7). However, a deeper understanding of the underlying mechanisms that govern immune detection of cancer cells is needed. In the present study, we aimed to increase our understanding of calreticulin (CRT) translocation, a necessary event for cancer cells to be recognized by the immune system (8), and how the nerve growth factor (NGF), a pro-angiogenic molecule overexpressed in EOC (9), participates in this process.

Several processes and signaling pathways are altered in a cancer cell, including angiogenesis (10). Angiogenesis is induced to provide the tumor with neo-vasculature, giving cancer cells access to sustenance and oxygen. During tumor progression, cancer cells undergo an 'angiogenic switch',

---

*Correspondence to:* Dr Carmen Aurora Romero, Laboratory of Endocrinology and Reproduction Biology, Clinical Hospital, University of Chile, Santos Dumont 999, Independencia, Santiago, Chile  
E-mail: cromero@hcuch.cl

*Abbreviations:* CRT, calreticulin; NGF, nerve growth factor; Tg, thapsigargin; Mtx, mitoxantrone; ER, endoplasmic reticulum

*Key words:* calreticulin, nerve growth factor, endoplasmic reticulum stress, calreticulin translocation, epithelial ovarian cancer

characterized by increased expression of pro-angiogenic molecules (11). The normal active ovary undergoes angiogenesis at regular intervals; in ovarian cancer, there are disturbances in the normal angiogenic regulation, including alteration of the proangiogenic molecules such as NGF and the vascular endothelial growth factor (VEGF) expression. Besides, the normal ovary expresses NGF and TRKA in granulosa cells, and NGF induces the proliferation of granulosa and theca cells (12). On the other hand, NGF levels are elevated and induce angiogenesis through its high affinity receptor TRKA by acting directly on endothelial cells and by stimulating VEGF production in epithelial cells in EOC (12). Besides, NGF induces proliferation and survival of EOC cells (13).

Tumor development is also accompanied by changes in the tumor's microenvironment (14,15). These changes can lead to the accumulation of misfolded and unfolded proteins in the endoplasmic reticulum (ER) lumen, inducing ER stress and eliciting the unfolded protein response (UPR) (16). In solid tumors the UPR promotes proliferation, survival, growth, migration and metastasis (17,18). Several ER stress sensors are responsible for UPR implementation, including PERK. Under ER stress conditions, PERK is phosphorylated and induces the phosphorylation of eIF2 $\alpha$  (19).

The PERK/eIF2 $\alpha$  branch of the UPR is important in CRT translocation (20). CRT is an ER resident that can also be present in other cell compartments, such as the cytosol, the nucleus (21), the cell membrane (22) and the extracellular space (23). CRT levels are increased in several types of cancer (23). This protein appears to have a dual role in cancer: on the one hand, it has a direct tumorigenic effect by inducing proliferation, migration and metastasis (24-26) and on the other, CRT is a potent anti-angiogenic molecule (27). Besides, when present on the cell surface, CRT triggers an anticancer immune response (8). Calreticulin translocation is induced by several chemotherapeutic agents through a pathway that involves the activation of the PERK/eIF2 $\alpha$  branch of the UPR (28).

NGF suppresses ER stress-mediated responses (29,30), but there is no information on whether it can also alter CRT translocation. In a previous study, we found that NGF induces an increase in CRT levels in human ovarian cancer cells (31). In the present study, we first evaluated the ovarian cancer cells ability to translocate CRT under ER and chemotherapeutic stress conditions. We then evaluated whether NGF alters stress-induced CRT translocation. We found that cancer cells translocate CRT from the ER to the cell surface upon induction of both ER and chemotherapeutic stress, suggesting a potential benefit for cancer patients, given the ability of the immune system to recognize and destroy cancer cells with exposed CRT. Notably, we found that NGF can prevent CRT translocation induced by chemotherapeutic stress, but it has no effect on CRT translocation after induction of direct ER stress. Given the elevated levels of NGF in cancer patients, this result could yield valuable information for the design of novel cancer treatment options.

## Materials and methods

*Tissue samples.* Ovarian tissues were obtained from Hospital Clínico, Universidad de Chile. Patients signed an informed

consent, which was approved by the Hospital's Ethics Committee. Normal ovarian samples (N-Ov) were obtained from women subjected to hysterectomy with oophorectomy due to non-ovarian pathologies. Ovarian tissues were also obtained from women diagnosed with ovarian tumors, both benign (Be-T) and borderline (Bo-T). Differentiation of serous epithelial ovarian cancer tissues samples was classified as: well (EOC I), moderate (EOC II) or poor (EOC III). An experienced pathologist performed the classification of each sample.

*Cell culture.* A2780 epithelial ovarian cancer cells were maintained in Dulbecco's modified Eagle's essential medium supplemented with Ham's F12 Nutrient Mixture (DMEM/HamF12; Sigma-Aldrich, St. Louis, MO, USA) with 10% fetal bovine serum (FBS; Hyclone™/Thermo Fisher Scientific, Rochester, NY, USA). All media contained 100 U/ml penicillin and 100  $\mu$ g/ml streptomycin (Hyclone™/Thermo Fisher Scientific). Cells were kept in a humidified incubator with 5% CO<sub>2</sub> at 37°C; medium was changed every 48 h.

*Cell treatments.* A2780 cells (1x10<sup>6</sup>) were treated with 100 ng/ml of NGF (Sigma-Aldrich), 1  $\mu$ M of thapsigargin (Abcam, Cambridge, UK) or 1  $\mu$ M of mitoxantrone (Sigma-Aldrich) for 4 h, or with 100 ng/ml NGF for 2 h followed by thapsigargin or mitoxantrone. NGF concentration was chosen according to previous results by our group (9,31,32); thapsigargin and mitoxantrone concentrations were chosen because of previous publications showing their effect on CRT localization (33-35). Cells were either scrapped and collected with lysis buffer for western blot analysis, trypsinized and collected with sterile Dulbecco's phosphate-buffered saline (DPBS; Gibco-Invitrogen, Camarillo, CA, USA) for flow cytometry analysis, or the cells fixed with paraformaldehyde for immunofluorescence experiments.

*Western blot analysis.* Cells were scrapped and homogenized in RIPA lysis buffer (50 mM Tris-Base, 150 mM NaCl, 0.5% sodium deoxycholate, 1% Triton X-100 and 0.1% sodium dodecyl sulfate); 1X protease and phosphatase inhibitor cocktail (Thermo Fisher Scientific) was added. After 20 min of centrifugation at 10,000 x g at 4°C, the supernatant was collected and protein concentration was determined using the BCA protein assay kit (Thermo Fisher Scientific). Proteins (50  $\mu$ g) were mixed with an equal amount of loading buffer, boiled and loaded into an 8, 10 or 12% resolving SDS-PAGE gel. After electrophoresis, proteins were transferred to a nitrocellulose membrane and blocked with Tris-buffered solution (20 mM Tris, pH 7.5; 137 mM NaCl; 0.1%) containing 0.1% Tween-20 (TTBS) and either 5% fat-free milk or 5% BSA. Afterwards, membranes were incubated overnight in primary antibody in either 5% milk in TTBS or 5% BSA in TTBS at 4°C, washed, and then incubated in HRP-labeled secondary antibody (1:5,000; KPL, Gaithersburg, MD, USA) for 1 h at room temperature. Signal detection was achieved with an enhanced chemiluminescence substrate, Western Lightning Plus-ECL (Perkin-Elmer, Waltham, MA, USA). Membranes were treated with stripping solution (25 mM glycine-HCl, pH 2.2, containing 1% w/v SDS and 1% v/v Tween-20) and re-probed with the primary antibody. Band intensities were measured densitometrically using ImageJ Image software

(National Institutes of Health, Bethesda, MD, USA). Relative band densities were normalized to  $\beta$ -actin as a loading control or to the appropriate total protein for phosphorylated proteins. The control condition was set to 1. Antibodies and dilutions used are as follows: p-eIF2 $\alpha$  (monoclonal rabbit anti-human, #9721, 1:500; Cell Signaling Technology, Danvers, MA, USA), t-eIF2 $\alpha$  (mouse monoclonal anti-human #2103, 1:1,000; Cell Signaling Technology), p-PERK (rabbit polyclonal anti-human, sc-32577, 1:250; Santa Cruz Biotechnology, Santa Cruz, CA, USA), t-PERK (rabbit monoclonal anti-human, #3192, 1:1,000; Cell Signaling Technology), CRT (mouse monoclonal anti-human, 1:1,000; BD Biosciences, San Jose, CA, USA),  $\beta$ -actin (monoclonal mouse anti-human, 1:10,000; Sigma-Aldrich).

**Flow cytometry.** CRT expression on the cell surface was determined by flow cytometry. Cells were trypsinized and suspended in medium with 10% FBS. After washing with 1X PBS, cells were blocked with 1X PBS containing 0.5% BSA and then stained with phycoerythrin (PE)-conjugated anti-CRT (monoclonal anti-human, ab83220, 1:200; Abcam) in 1X PBS with 0.5% BSA at 4°C for 30 min, away from light. After washing with 1X PBS, stained cells were analyzed in a flow cytometer (LSRFortessa™ X-20 cell analyzer; BD Biosciences) and the data were processed with FlowJo software (Tree Star, Inc., Ashland, OR, USA). Results were expressed as mean fluorescence intensity (MFI); the control condition was set to 1.

**Immunofluorescence.** Cells were grown and treated in Lab-Tek chambers (Thermo Scientific™ Nunc™ Lab-Tek™ II Chamber Slide™ System). Next, treated cells were fixed with 4% paraformaldehyde in PBS for 15 min at room temperature. Cells were then permeabilized with triton 0.3% for 10 min, blocked with 5% BSA in PBS for 10 min and then incubated with 1:10,000 rabbit anti-human calreticulin (CRT) antibody and anti-KDEL antibody (mouse monoclonal anti-human, #12223, 1:500; Abcam) overnight. Another group of cells was incubated for 1 h with wheat germ agglutinin (WGA, W11261, 1:1,000; Thermo Fisher Scientific) for membrane staining immediately after fixation, and then blocked and incubated with 1:10,000 rabbit anti-human CRT, with no previous permeabilization step. Afterwards, all cells were washed and incubated with Alexa Fluor 594 conjugated anti-rabbit secondary antibody (#8889; Cell Signaling Technology) and Alexa Fluor 488 conjugated with anti-mouse secondary antibody (#4408; Cell Signaling Technology) at 1:500 for 1 h. Cells were mounted in mounting medium with DAPI (ProLong® Gold Antifade reagent with DAPI; Cell Signaling Technology) and observed under a confocal microscope (Zeiss LSM 700).

**Image analysis.** Immunofluorescence pictures were deconvoluted with the Huygens software (Scientific Volume Imaging, Hilversum, The Netherlands). Mean fluorescence intensity (MFI) was determined with ImageJ software. In order to evaluate fluorescence intensity across one cell, a line was traced and green and red fluorescence intensity was determined in that line.

**Statistical analysis.** Results are expressed as mean  $\pm$  SEM. Normality was determined by the Kolmogorov-Smirnov

test. Significant differences between groups were assessed by one-way analysis of variance (ANOVA) followed by a Bonferroni post test in case of parametric data, and by Kruskal Wallis followed by Dunn's post test in case of non-parametric distribution.  $P < 0.05$  were considered statistically significant. The statistical analysis was done with GraphPad Prism 5 software (Graphpad Software, Inc., La Jolla, CA, USA).

## Results

*Reticulum and cytotoxic stress induce CRT exposure to the cell surface in A2780 ovarian cancer cells.* A2780 cells were treated for 4 h with thapsigargin (Tg), a reticulum stress inducer, or mitoxantrone (Mtx), a cytotoxic chemotherapeutic agent. Both compounds modified the CRT subcellular localization, as determined with confocal microscopy. In basal conditions CRT is found with a perinuclear distribution in A2780 cells, as shown in Fig. 1A-a, concordant with ER localization. CRT is shown in red, the nucleus is shown in blue and the cell membranes were stained in green. These cells were not permeabilized, however, paraformaldehyde fixation causes loss of cell membrane integrity, inducing partial permeabilization (36). Therefore, it is possible to detect intracellular CRT. Cell membranes were stained with WGA, which marks both the cell surface membrane and intracellular membranes. After Tg and Mtx stimuli, CRT cell distribution changes, and CRT can be detected in the cell periphery (Fig. 1A-b and A-c). These experiments were also done in triton-permeabilized cells. In this case, cells were also stained with an anti-KDEL antibody. KDEL is a peptide sequence found in ER proteins. CRT also has a KDEL sequence. CRT was marked with red fluorescence and KDEL was visualized in green (Fig. 1B). Since cells were permeabilized, the red and green marks correspond exclusively to intracellular staining. Fluorescence intensity for CRT (red line) and KDEL (green line) was measured along the line drawn in white. Under basal conditions (Fig. 1B-a2), the KDEL and CRT intensity signals are similar, indicating that CRT is mostly found in the ER, along with other KDEL proteins. After Tg or Mtx incubation, KDEL intensity is higher than CRT intensity near the nucleus, indicating that CRT has left the ER, leaving behind the other KDEL-bearing proteins (Fig. 1B-b2 and c2). All the above results suggest that Tg and Mtx are inducing CRT translocation; however, given the loss of membrane integrity due to paraformaldehyde fixing and to give more strength to the 2D plots, flow cytometry experiments were carried out to verify the CRT expression on the cell surface. Since flow cytometry is done on live cells that have intact membrane integrity, this technique allows for CRT staining exclusively on the cell surface. As seen in Fig. 1C-a, after Tg or Mtx treatments, CRT expression increased on the cell surface, expressed by a shift to the right: blue line for Tg, green line for Mtx, compared to the red basal line. CRT levels in the cell surface were also expressed as mean fluorescence intensity (MFI). As seen in Fig. 1C-b, MFI increases after Tg or Mtx treatment, which represents an increase in CRT translocation to the cell surface.

*NGF increases CRT levels with no sub-localization change.* Next, we determined the effect of the pro-angiogenic and pro-carcinogenic NGF molecule on CRT levels and subcellular

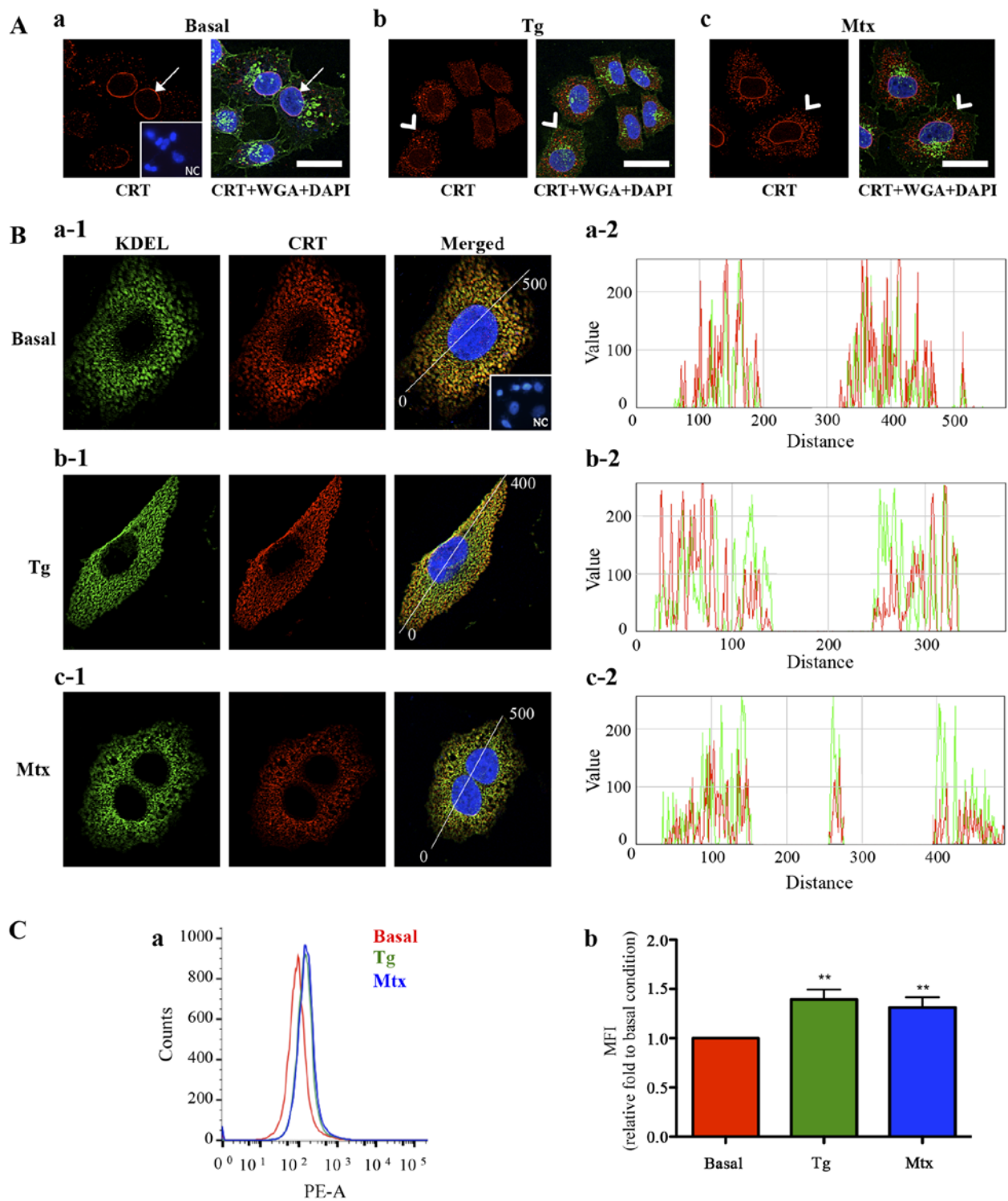


Figure 1. Tg and Mtx induce CRT exposure in A2780 cells. (A) Immunofluorescence analysis of non-permeabilized A2780 cells treated with Tg or Mtx. CRT signal is shown in red. Cell membranes were stained with WGA (green) and nuclei are marked with DAPI (blue). Arrows point to CRT with perinuclear distribution; arrowheads indicate CRT in the cell periphery. Scale bar, 50  $\mu$ m. (B) Cells were permeabilized with triton and CRT signal was merged with that of an ER marker, KDEL. The diagrams on the right show CRT signal intensity (red) and KDEL intensity (green) along the yellow line drawn in one representative cell. (C) Surface expression levels of CRT after Tg and Mtx treatment were determined by flow cytometry. PE, phycoerythrin. The graph illustrates mean fluorescence intensity (MFI) averaged over four experiments; the basal condition was normalized to 1; \*\* $P < 0.01$  compared to basal; the error bars denote SEM. NC, negative control, without primary antibody.

localization in A2780 cells. After 4 h of incubation with NGF, we found an increase of CRT protein levels, measured by western blot analysis (Fig. 2A). A semi-quantitative analysis of CRT fluorescence intensity after NGF treatment, seen in

Fig. 2C, shows a similar result, treatment of A2780 cells with NGF induces an increase of CRT levels compared to the basal condition. However, NGF does not alter CRT subcellular localization, as seen in Fig. 2B. This agrees with flow cytometry

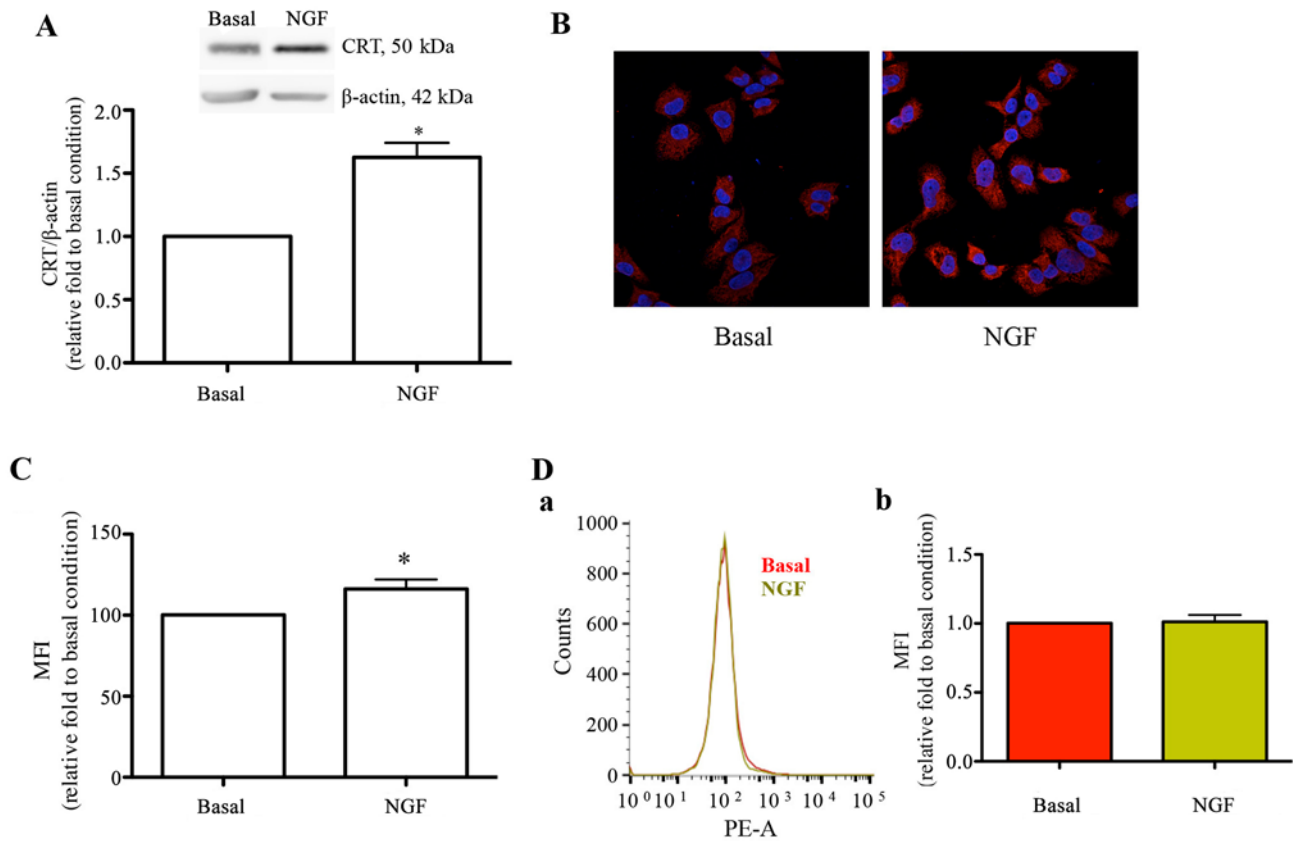


Figure 2. NGF induces an increase of intracellular CRT protein levels in A2780 cells. (A) Western blot analysis of CRT levels in A2780 cells treated with NGF;  $\beta$ -actin served as internal control. A representative image of the gel electrophoresis is shown. Results are the average of five separate experiments. (B) CRT was visualized in A2780 cells with immunofluorescence. CRT is shown in red and the nuclei were stained with DAPI and visualized in blue. (C) Quantitative data for the fluorescence intensity (MFI) of CRT was measured in order to semi-quantify CRT protein levels. Data are shown as averages of three experiments. (D) Surface expression levels of CRT after 4-h treatment with NGF (100 ng/ml) were determined by flow cytometry; the graph illustrates mean fluorescence intensity (MFI) averaged over four experiments. PE, phycoerythrin. The error bars denote SEM; basal conditions were normalized to 1; \* $P < 0.05$  compared to basal.

experiments, as seen in the histogram in Fig. 2D-a: the line representing the basal condition (red) and the line denoting NGF treatment (yellow) are similar. These results were also expressed as MFI (mean fluorescence intensity) (Fig. 2D-b), and no change is detected between basal and NGF-treated cells. These flow cytometry results indicate that after NGF treatment CRT is not being transported to the cell periphery.

*NGF pre-incubation inhibits Mtx-induced CRT exposure to the cell surface in A2780 ovarian cancer cells.* The ER stress response is necessary for CRT exposure to the cell surface and NGF can alter the ER stress response. In order to investigate the effect of NGF on CRT translocation, A2780 cells were incubated with NGF for 2 h previous to Tg or Mtx treatment. In the histogram shown in Fig. 3A-a, Mtx treatment is expressed as a dotted line, and it is shifted to the right, as compared to the basal condition (solid line), indicating that CRT was transported to the cell surface after Mtx treatment. NGF inhibited this shift (dashed line), meaning that CRT remained inside the cell. In Fig. 3A-b these results are expressed as MFI. However, NGF had no effect in CRT translocation to the cell surface after Tg treatment, as seen in the histogram in Fig. 3B-a: the dashed line, representing NGF-treated cells before Tg incubation, did not shift compared to the basal condition (solid line). Fig. 3B-b shows the MFI analysis. In summary, NGF inhibited

CRT translocation induced by Mtx (Fig. 3A); nevertheless, NGF had no effect on Tg-induced CRT translocation (Fig. 3B).

*NGF alters the UPR induced by cytotoxic stress.* CRT translocation requires the activation of the PERK/eIF2 $\alpha$  branch from the UPR pathway, which is activated after ER stress. Activation of PERK/eIF2 $\alpha$  was evaluated as p-PERK and p-eIF2 $\alpha$  by western blot analysis. Representative gels of PERK and p-PERK are shown in Fig. 4A and B. When A2780 cells were treated with Tg, an increase was found in p-PERK. However, in cells previously treated with NGF, a significant inhibition of this activation was found, as shown in the semi-quantitative analysis of the western blot analysis (Fig. 4A). Results similar to those obtained with p-PERK were found in A2780 cells treated with Mtx alone or with Mtx after treatment with NGF, as shown in Fig. 4B.

Representative gel images of eIF2 $\alpha$  and p-eIF2 $\alpha$  are shown in Fig. 4C and D. In a semi-quantitative analysis of eIF2 $\alpha$  activation in A2780 cells treated with Tg, we found a significant increase of p-eIF2 $\alpha$ , however, pre-incubation with NGF did not change the activation of p-eIF2 $\alpha$  after Tg treatment (Fig. 4C). In A2780 treated with Mtx we found a significant increase of p-eIF2 $\alpha$ , and this activation was diminished by previous NGF treatment (Fig. 4D). These results agree with the flow cytometry experiments, since NGF pre-incubation could

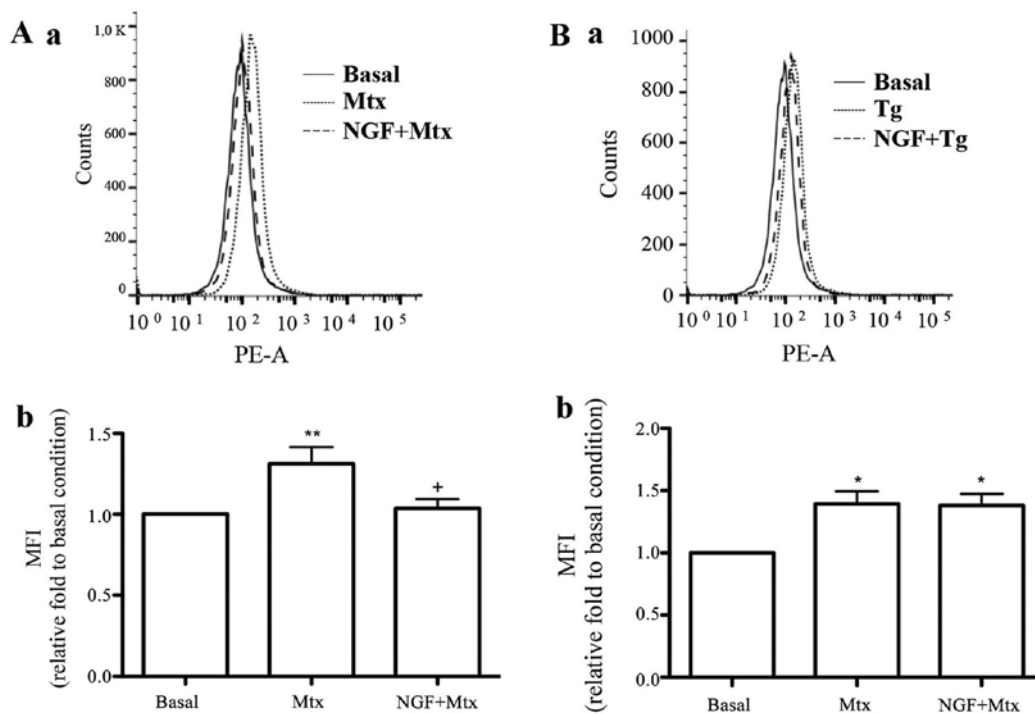


Figure 3. Flow cytometric analysis of surface CRT in Tg and Mtx treated A2780 cells after NGF incubation. Cells were incubated with NGF. Afterwards, cells were treated with either Mtx (A) or Tg (B). Surface expression of CRT on the cell surface was measured by flow cytometry. The graph illustrates mean fluorescence intensity (MFI) averaged over four experiments; the basal condition was normalized to 1; \* $P < 0.05$  compared to basal; \*\* $P < 0.01$  compared to basal; + $P < 0.05$  compared to the Mtx-treated group. PE, phycoerythrin. The error bars denote SEM.

only inhibit Mtx-induced CRT exposure to the cell surface, having no effect on CRT expression on the cell surface after Tg stimulation. Moreover, these results suggest that NGF could interfere in the Mtx actions when this compound is used as a therapeutic drug.

Tg and Mtx did not change CRT total levels (Fig. 4E and F). CRT is a 50-kDa protein that has been shown to migrate at 60 kDa in SDS-PAGE gels (37,38). NGF, on the other hand, did not change the active levels of either PERK or eIF2 $\alpha$  (Fig. 4A and B, respectively), but it did induce an increase in CRT protein levels (Fig. 4E and F).

*NGF prevents cell death induced by a chemotherapeutic drug.* Mtx is a drug used against cancer given its capacity to induce cell death. Because of the NGF ability to inhibit the UPR induced by Mtx (Fig. 4B and D), we decided to evaluate whether NGF has also an effect on cell death after Mtx treatment. Cells were incubated for 48 h with either Mtx or with NGF and Mtx and then cell viability was measured. As seen in Fig. 5, cells that were treated with both NGF and Mtx had a higher survival rate compared to cells treated with Mtx alone.

*CRT levels and the UPR are altered in human ovarian samples.* In order to better understand how these processes work in human ovarian cancer, we evaluated whether protein levels of CRT, PERK and/or eIF2 $\alpha$  were altered in human ovarian cancer samples. As shown in Fig. 6, we found an increase in CRT levels in EOC II and EOC III as compared to normal inactive ovaries. p-PERK levels were also elevated in EOC as compared to normal ovaries. Notably, p-eIF2 $\alpha$  levels were higher in EOC II than in less differentiated samples.

## Discussion

CRT is a multifunctional, buffering and ubiquitous protein mainly involved in protein folding and the maintenance of calcium homeostasis (39). CRT is also involved in the pathogenesis of several diseases, including different types of cancer (40). In cancer cells exposed to reticulum and/or cytotoxic stress, CRT is translocated from the ER to the cell membrane, where it induces an anti-immune response against cancer cells. This immune response reduces or even destroy the tumor (28).

In human ovarian cancer cells, we found that thapsigargin (Tg) and mitoxantrone (Mtx) induce CRT translocation from the ER to the cell surface (Fig. 1). Tg, a compound that inhibits ER calcium pumps (41), induces a direct ER stress response that we found to be mediated by the activation of the UPR. Mtx, on the other hand, is an anticancer drug with DNA binding properties that induces cell death, while generating ER stress in an indirect manner (42). We found that both of these compounds stimulate CRT translocation from the ER to the cell surface (Fig. 1), which could indicate that ovarian cancer cells have the potential to respond to immunotherapy.

Despite the ability of CRT to induce an anticancer immune response, it has also been associated with pro-carcinogenic properties (40). CRT has been found to be elevated in several types of cancer (39), although no evidence of efficient translocation to the tumor cell surface has been presented. One of CRT properties is related to angiogenesis, a necessary process for the survival of solid tumors (25). In ovarian cancer, characterized by high levels of angiogenesis, this process is mostly driven by VEGF, a pro-angiogenic molecule overexpressed

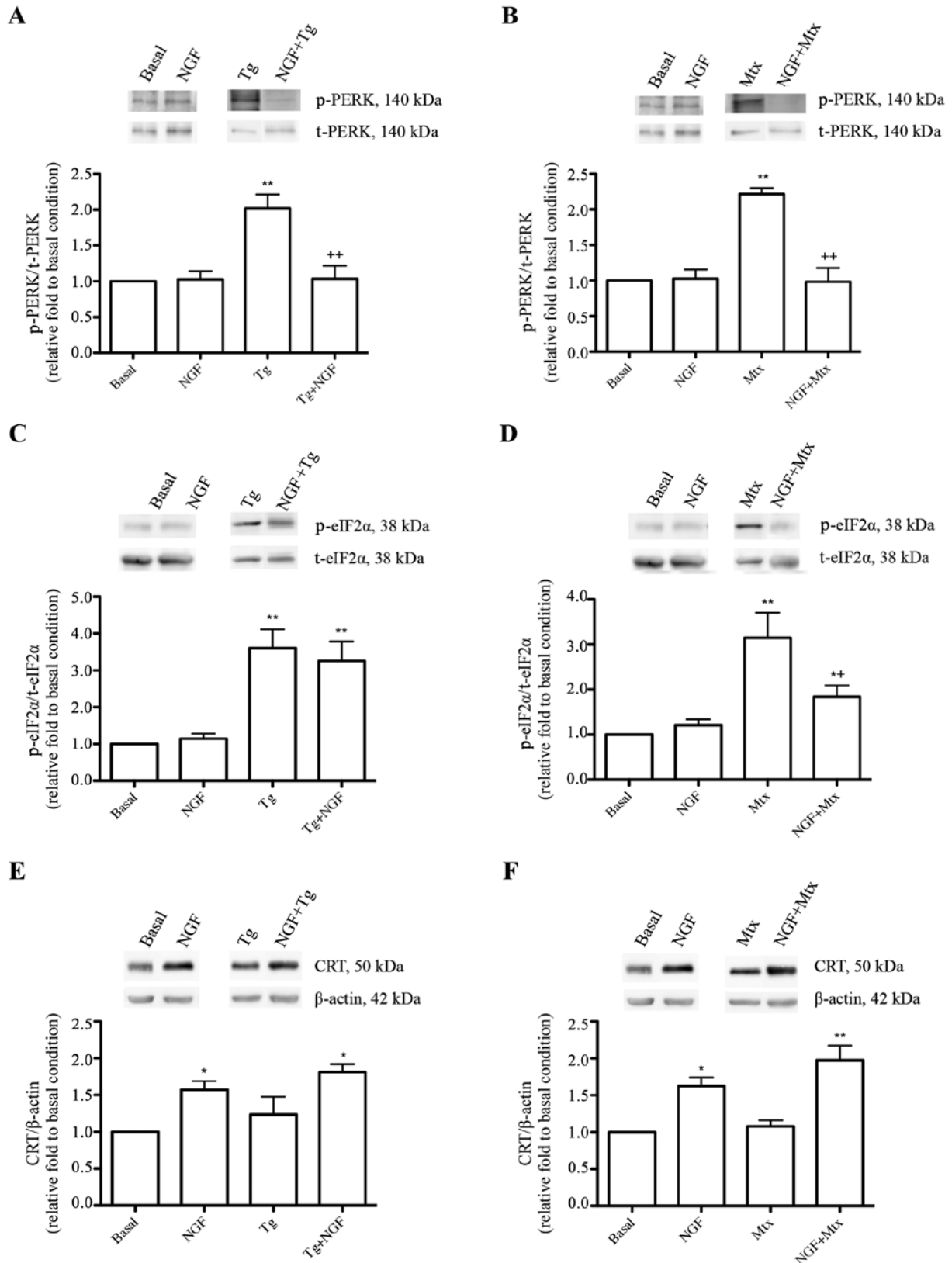


Figure 4. Mtx, Tg and NGF effect on PERK, eIF2 $\alpha$  and CRT protein levels in A2780 cells. (A) Western blot analysis of PERK levels in A2780 cells treated with NGF, Tg or pre-treated with NGF before Tg treatment. Results are expressed as phosphorylated protein in relation to the total form. (B) Western blot analysis of PERK levels in A2780 cells treated with NGF, Mtx or pre-treated with NGF before Mtx treatment. Results are expressed as phosphorylated protein in relation to total. (C) Western blot analysis of eIF2 $\alpha$  levels in A2780 cells treated with NGF, Tg, or pre-treated with NGF before Tg treatment. Results are expressed as phosphorylated protein in relation to total. (D) Western blot analysis of eIF2 $\alpha$  levels in A2780 cells treated with NGF, Mtx (1 mM) or pre-treated with NGF before Mtx treatment. Results are expressed as phosphorylated protein in relation to total. (E) Western blot analysis of CRT levels in A2780 cells treated with NGF, Tg or pre-treated with NGF before Tg treatment;  $\beta$ -actin served as internal control. (F) Western blot analysis of CRT levels in A2780 cells treated with NGF, Mtx or pre-treated with NGF before Mtx treatment;  $\beta$ -actin served as internal control. In all images, a representative image of the gel electrophoresis is shown. Results are the average of five separate experiments. The error bars denote SEM; basal conditions were normalized to 1; \*P<0.05 compared to basal; \*\*P<0.01 compared to basal; \*P<0.05; \*\*P<0.01 compared to the Tg-treated condition.

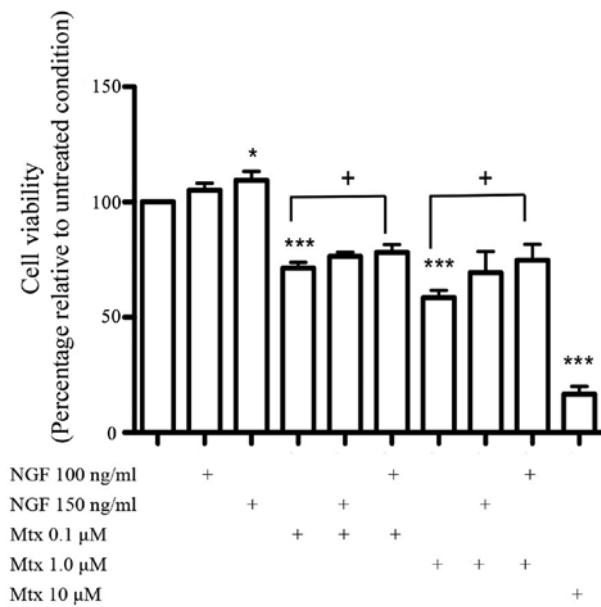


Figure 5. NGF prevents Mtx-induced cell death. Cells were plated in 96-well cell culture plates and incubated with, Mtx, or both. Mtx was used as a positive control for cell death. Viability was measured using a colorimetric assay. \* $P < 0.05$ ; \*\*\* $P < 0.001$  compared to the control; + $P < 0.05$  as indicated. Results are the average of three experiments done in quintuplicates.

in most solid tumors (43). Another pro-angiogenic molecule overexpressed in ovarian cancer is NGF, which acts directly on endothelial cells and also on cancer cells, inducing them to increase their VEGF expression and secretion (12). In the present study, we found that NGF increases CRT levels (Fig. 2), which could be associated with pro-carcinogenic properties; however, CRT effects in cancer seem to be dependent on its subcellular localization. We found that NGF induces an increase of CRT protein levels; however, this increase is not accompanied by a change on its subcellular localization: CRT is maintained inside the cell (Fig. 2). As a consequence, CRT would be promoting angiogenesis and other pro-carcinogenic processes instead of inducing an anticancer immune response.

CRT translocation is mediated by the activation of the reticulum stress response, specifically the UPR branch involving the phosphorylation of PERK and its substrate, eIF2 $\alpha$  (28). NGF has been found to inhibit the effects of reticulum stress, including reducing apoptosis after UPR activation (29,30). In this study, we determined that NGF also reduced Mtx-induced CRT exposure to the cell membrane (Fig. 3). This is an interesting result, given the high levels of NGF normally found in ovarian cancer. If NGF inhibits CRT transport from the ER to the cell membrane in ovarian cancer patients, this could mean that an anti-immune therapy based on chemotherapeutic drugs that induce this CRT translocation would be less efficient in these women than for patients suffering from other types of cancer.

NGF, on the other hand, did not affect the ability of Tg to induce a change in CRT sub-cellular localization (Fig. 3). This is consistent with the results obtained in the western blot analysis, as NGF was unable to prevent eIF2 $\alpha$  phosphorylation induced by Tg. Both Mtx and Tg induced the UPR, a necessary step for CRT translocation; NGF, however, inhibited this response when induced by Mtx, while it only partially inhibited

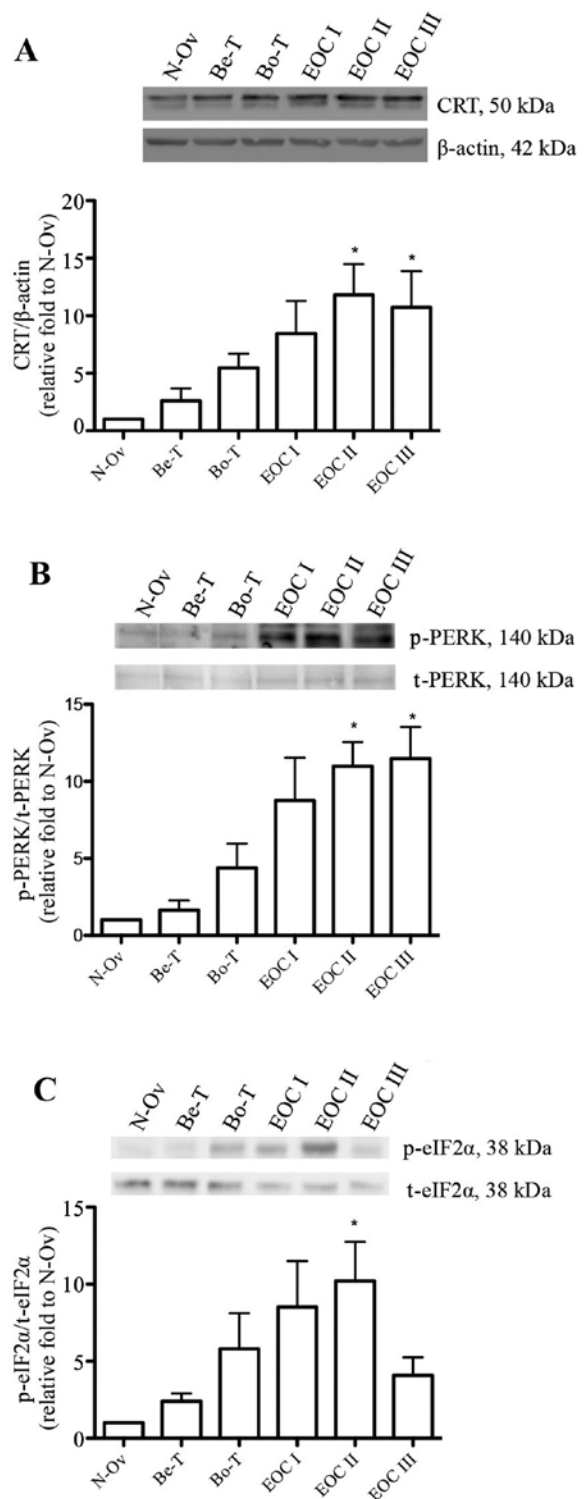


Figure 6. CRT, PERK and eIF2 $\alpha$  protein levels in ovarian human samples. Western blot analyses were done in order to measure (A) CRT (B) PERK and (C) eIF2 $\alpha$  protein levels in human ovarian samples. N-Ov, normal inactive ovaries; Be-T, benign tumors; Bo-T, borderline tumors; EOC I, well differentiated epithelial ovarian cancer; EOC II, moderately differentiated epithelial ovarian cancer; EOC III, poorly differentiated epithelial ovarian cancer. Results are expressed as phosphorylated protein in relation to total or with  $\beta$ -actin served as internal control. In all images, a representative image of the gel electrophoresis is shown. The error bars denote SEM; the inactive normal ovary was normalized to 1; \* $P < 0.05$  compared to N-Ov.

Tg effect, as eIF2 $\alpha$  was still phosphorylated (Fig. 4). This could be explained by the existence of other pathways induced by Tg,

including the activation of oxidative stress, which also induces eIF2 $\alpha$  phosphorylation and CRT translocation to the cell periphery. In a therapeutic setting, this result could point to the advantage of accompanying chemotherapeutic treatment with a direct induction of the ER stress response, given its effect on CRT translocation, despite the participation of NGF.

Because of the NGF effect on the Mtx-induced UPR, we sought to determine if NGF had an effect on cell death induced by Mtx. Indeed, NGF diminished cell death after treatment with this cytotoxic agent (Fig. 5). Mtx is used in epithelial ovarian cancer; therefore, we sought to evaluate the effect of NGF on Mtx cytotoxicity.

In order to gain a better understanding of these processes in human ovarian cancer, we measured the UPR and CRT protein levels in six groups of frozen human ovary samples: normal inactive ovaries, benign tumors, borderline tumors and EOC I, EOC II and EOC III (respectively corresponding to well, moderately and poorly differentiated epithelial ovarian cancers). We found that CRT is increased in advanced stages of epithelial ovarian cancer, matching other reports in both ovarian cancer and other types of cancer (23). We also found an increase in p-PERK and p-eIF2 $\alpha$  levels, consistent with the characteristic ER stress inducing microenvironment that surrounds most tumors. However, eIF2 $\alpha$  is reduced in advanced cancer samples, which could be an impediment to CRT translocation. It is possible that cancer cells adapt to ER stress, which in turn could lead to the inhibition of CRT transport to the cell surface.

The induction of CRT translocation from the ER to the cell surface through the use of cytotoxic drugs is a novel strategy for the treatment of cancer (28). However, in this study we found that NGF inhibits CRT movement. Further studies should determine whether NGF can alter immune recognition and destruction of cancer cells, and the role of ER stress inducers in increasing the efficiency of immunotherapy against ovarian cancer.

## Acknowledgements

The present study was supported by grants #1110372 and #1160139 from the Fondo Nacional de Desarrollo Científico y Tecnológico, Chile (to C.R.), the #1130099 grant from the Fondo Nacional de Desarrollo Científico y Tecnológico, Chile (to A.F.) and the #21120252 grant from the Comisión Nacional de Ciencia y Tecnología, Chile (to C.V.).

## References

- Torre LA, Bray F, Siegel RL, Ferlay J, Lortet-Tieulent J and Jemal A: Global cancer statistics, 2012. *CA Cancer J Clin* 65: 87-108, 2015.
- Baldwin LA, Huang B, Miller RW, Tucker T, Goodrich ST, Podzielinski I, DeSimone CP, Ueland FR, van Nagell JR and Seamon LG: Ten-year relative survival for epithelial ovarian cancer. *Obstet Gynecol* 120: 612-618, 2012.
- Sopik V, Iqbal J, Rosen B and Narod SA: Why have ovarian cancer mortality rates declined? Part I. Incidence. *Gynecol Oncol* 138: 741-749, 2015.
- Cuellar-Partida G, Lu Y, Dixon SC, Fasching PA, Hein A, Burghaus S, Beckmann MW, Lambrechts D, Van Nieuwenhuysen E, Vergote I, *et al*: Australian Ovarian Cancer Study: Assessing the genetic architecture of epithelial ovarian cancer histological subtypes. *Hum Genet* 135: 741-756, 2016.
- Jayson GC, Kohn EC, Kitchener HC and Ledermann JA: Ovarian cancer. *Lancet* 384: 1376-1388, 2014.
- Papaioannou NE, Beniata OV, Vitsos P, Tsitsilonis O and Samara P: Harnessing the immune system to improve cancer therapy. *Ann Transl Med* 4: 261-276, 2016.
- Knutson KL, Karyampudi L, Lamichhane P and Preston C: Targeted immune therapy of ovarian cancer. *Cancer Metastasis Rev* 34: 53-74, 2015.
- Obeid M, Tesniere A, Ghiringhelli F, Fimia GM, Apetoh L, Perfettini JL, Castedo M, Mignot G, Panaretakis T, Casares N, *et al*: Calreticulin exposure dictates the immunogenicity of cancer cell death. *Nat Med* 13: 54-61, 2007.
- Tapia V, Gabler F, Muñoz M, Yazigi R, Paredes A, Selman A, Vega M and Romero C: Tyrosine kinase A receptor (trkA): A potential marker in epithelial ovarian cancer. *Gynecol Oncol* 121: 13-23, 2011.
- Hanahan D and Weinberg RA: Hallmarks of cancer: The next generation. *Cell* 144: 646-674, 2011.
- Yadav L, Puri N, Rastogi V, Satpute P and Sharma V: Tumour angiogenesis and angiogenic inhibitors: A review. *J Clin Diagn Res* 9: XE01-XE05, 2015.
- Vera C, Tapia V, Vega M and Romero C: Role of nerve growth factor and its TRKA receptor in normal ovarian and epithelial ovarian cancer angiogenesis. *J Ovarian Res* 10: 7: 82, 2014
- Urzua U, Tapia V, Geraldo MP, Selman A, Vega M and Romero C: Nerve growth factor stimulates cellular proliferation of human epithelial ovarian cancer. *Horm Metab Res* 44: 656-661, 2012.
- Bussard KM, Mutkus L, Stumpf K, Gomez-Manzano C and Marini FC: Tumor-associated stromal cells as key contributors to the tumor microenvironment. *Breast Cancer Res* 18: 84, 2016.
- Balkwill FR, Capasso M and Hagemann T: The tumor microenvironment at a glance. *J Cell Sci* 125: 5591-5596, 2012.
- Mahdi AA, Rizvi SH and Parveen A: Role of endoplasmic reticulum stress and unfolded protein responses in health and diseases. *Indian J Clin Biochem* 31: 127-137, 2016.
- Mori K: The unfolded protein response: The dawn of a new field. *Proc Jpn Acad, Ser B Physiol Sci* 91: 469-480, 2015.
- Vandewynckel YP, Laukens D, Geerts A, Bogaerts E, Paridaens A, Verhelst X, Janssens S, Heindryckx F and Van Vlierberghe H: The paradox of the unfolded protein response in cancer. *Anticancer Res* 33: 4683-4694, 2013.
- Sovolyova N, Healy S, Samali A and Logue SE: Stressed to death: mechanisms of ER stress-induced cell death. *Biol Chem* 395: 1-13, 2014.
- Yang Y, Li XJ, Chen Z, Zhu XX, Wang J, Zhang LB, Qiang L, Ma YJ, Li ZY, Guo QL, *et al*: Wogonin induced calreticulin/annexin A1 exposure dictates the immunogenicity of cancer cells in a PERK/AKT dependent manner. *PLoS One* 7: e50811, 2012.
- Holaska JM, Black BE, Love DC, Hanover JA, Leszyk J and Paschal BM: Calreticulin Is a receptor for nuclear export. *J Cell Biol* 152: 127-140, 2001.
- Ramesh BS, Giorgakis E, Lopez-Davila V, Dashtarzheneha AK and Loizidou M: Detection of cell surface calreticulin as a potential cancer biomarker using near-infrared emitting gold nanoclusters. *Nanotechnology* 27: 285101, 2016.
- Lu YC, Weng WC and Lee H: Functional roles of calreticulin in cancer biology. *BioMed Res Int* 2015: 526524, 2015.
- Zamanian M, Qader Hamadneh LA, Veerakumarasivam A, Abdul Rahman S, Shohaimi S and Rosli R: Calreticulin mediates an invasive breast cancer phenotype through the transcriptional dysregulation of p53 and MAPK pathways. *Cancer Cell Int* 16: 56, 2016.
- Sheng W, Chen C, Dong M, Zhou J, Liu Q, Dong Q and Li F: Overexpression of calreticulin contributes to the development and progression of pancreatic cancer. *J Cell Physiol* 229: 887-897, 2014.
- Chiang WF, Hwang TZ, Hour TC, Wang LH, Chiu CC, Chen HR, Wu YJ, Wang CC, Wang LF, Chien CY, *et al*: Calreticulin, an endoplasmic reticulum-resident protein, is highly expressed and essential for cell proliferation and migration in oral squamous cell carcinoma. *Oral Oncol* 49: 534-541, 2013.
- Shu Q, Li W, Li H and Sun G: Vasostatin inhibits VEGF-induced endothelial cell proliferation, tube formation and induces cell apoptosis under oxygen deprivation. *Int J Mol Sci* 15: 6019-6030, 2014.
- Wiersma VR, Michalak M, Abdullah TM, Bremer E and Eggleton P: Mechanisms of translocation of ER chaperones to the cell surface and immunomodulatory Roles in cancer and autoimmunity. *Front Oncol* 5: 7, 2015.

29. Zhu SP, Wang ZG, Zhao YZ, Wu J, Shi HX, Ye LB, Wu FZ, Cheng Y, Zhang HY, He S, *et al*: Gelatin nanostructured lipid carriers incorporating nerve growth factor inhibit endoplasmic reticulum stress-induced apoptosis and improve recovery in spinal cord injury. *Mol Neurobiol* 53: 4375-4386, 2016.
30. Wei K, Liu L, Xie F, Hao X, Luo J and Min S: Nerve growth factor protects the ischemic heart via attenuation of the endoplasmic reticulum stress induced apoptosis by activation of phosphatidylinositol 3-kinase. *Int J Med Sci* 12: 83-91, 2015.
31. Vera C, Tapia V, Kohan K, Gabler F, Ferreira A, Selman A, Vega M and Romero C: Nerve growth factor induces the expression of chaperone protein calreticulin in human epithelial ovarian cells. *Horm Metab Res* 44: 639-643, 2012.
32. Campos X, Muñoz Y, Selman A, Yazigi R, Moyano L, Weinstein-Oppenheimer C, Lara HE and Romero C: Nerve growth factor and its high-affinity receptor trkA participate in the control of vascular endothelial growth factor expression in epithelial ovarian cancer. *Gynecol Oncol* 104: 168-175, 2007.
33. Martins I, Kepp O, Schlemmer F, Adjemian S, Tailler M, Shen S, Michaud M, Menger L, Gdoura A, Tajeddine N, *et al*: Restoration of the immunogenicity of cisplatin-induced cancer cell death by endoplasmic reticulum stress. *Oncogene* 30: 1147-1158, 2011.
34. Zuppini A, Groenendyk J, Cormack LA, Shore G, Opas M, Bleackley RC and Michalak M: Calnexin deficiency and endoplasmic reticulum stress-induced apoptosis. *Biochemistry* 41: 2850-2858, 2002.
35. Kepp O, Galluzzi L, Giordanetto F, Tesniere A, Vitale I, Martins I, Schlemmer F, Adjemian S, Zitvogel L and Kroemer G: Disruption of the PP1/GADD34 complex induces calreticulin exposure. *Cell Cycle* 8: 3971-3977, 2009.
36. Hobro AJ and Smith NI: An evaluation of fixation methods: Spatial and compositional cellular changes observed by Raman imaging. *Vib Spectrosc* (In press).
37. Milner RE, Baksh S, Shemanko C, Carpenter MR, Smillie L, Vance JE, Opas M and Michalak M: Calreticulin, and not calsequestrin, is the major calcium binding protein of smooth muscle sarcoplasmic reticulum and liver endoplasmic reticulum. *J Biol Chem* 266: 7155-7165, 1991.
38. Parmar T, Nimbkar-Joshi S, Katkam RR, Gadkar-Sable S, Chaudhari U, Manjramkar DD, Savardekar L, Jacob S, Puri CP and Sachdeva G: Differential expression of calreticulin, a reticuloplasm in primate endometrium. *Hum Reprod* 24: 2205-2216, 2009.
39. Wang WA, Groenendyk J and Michalak M: Calreticulin signaling in health and disease. *Int J Biochem Cell Biol* 44: 842-846, 2012.
40. Zamanian M, Veerakumarasivam A, Abdullah S and Rosli R: Calreticulin and cancer. *Pathol Oncol Res* 19: 149-154, 2013.
41. Bian JH, Ghosh TK, Wang JC and Gill DL: Identification of intracellular calcium pools. Selective modification by thapsigargin. *J Biol Chem* 15: 266: 8801-8806, 1991
42. Posner LE, Dukart G, Goldberg J, Bernstein T and Cartwright K: Mitoxantrone: An overview of safety and toxicity. *Invest New Drugs* 3: 123-132, 1985.
43. Jackson AL, Eisenhauer EL and Herzog TJ: Emerging therapies: Angiogenesis inhibitors for ovarian cancer. *Expert Opin Emerg Drugs* 20: 331-346, 2015.